J. Ullrich V.P. Shevelko (Eds.)

Many-Particle Quantum Dynamics in Atomic and Molecular Fragmentation

With 179 Figures

Springer

in: Many-Particle Quantum Dynamics in Atomic and Molecular Fragmentation, e.d. V.P. Shevelko, J. Ullrich, Springer-Verlag 2002

14

From Atoms to Molecules

R. Dörner, H. Schmidt-Böcking, V. Mergel, T. Weber, L. Spielberger, O. Jagutzki, A. Knapp, H.P. Bräuning

14.1 From Atoms to Molecules

14.1.1 Introduction

In the present chapter we discuss direct photo double ionization by single photon absorption (section 14.1.2) and Compton scattering (section 14.1.3). We do not discuss the closely related phenomenon of multiple ionization by two step processes such as photoionization followed by single or multiple Auger decay. We concentrate on the two most fundamental two electron target systems: the helium atom (sections 14.1.2 and 14.1.3) and molecular hydrogen (deuterium) (sections 14.1.4). The subject of photo double ionization of Helium is a mature field now in which an impressive experimental and theoretical breakthrough has been achieved in the previous 10 years. The theoretical progress is described in chapter 2 of this book, we therefore restrict ourselves here to a phenomenological description and intuitive interpretation of the physical phenomena. For the problem of two electron processes in molecules in contrast the major challenges for experimentalist and theoretician lie still ahead.

14.1.2 Double Ionization of Helium by Photo-Absorption

Energy, Momentum and Angular Momentum Considerations Double ionization of helium by photo-absorption becomes possible if the energy of the photon is higher than the sum of the binding energies of both electrons ($E_{ion}^{2+} = 24.6\,eV + 54.4\,eV = 79\,eV$). The excess energy $E_{\rm exc} = E_\gamma - E_{ion}^{2+}$ can be shared among the two electrons in the continuum $E_1 + E_2 = E_{exc}$. The energy of the He^{2+} nucleus is negligible due to its heavy mass. In momentum space however the momenta of the electrons and the nucleus are of the same order of magnitude. From momentum conservation we obtain (assuming the atom at rest in the initial state):

$$k_\gamma = k_1 + k_2 + k_{He^{2+}} \tag{14.1}$$

At non relativistic energies the photon momentum can be neglected against the electron and ion momenta ($k_\gamma \approx 0$). Hence in the final state the sum of the two electron momenta is balanced by the ion (see section **??** for a

more detailed discussion). At photon energies of below typically 1 keV the dipole approximation is expected to hold. Therefore, the absorption of the photon leads to $\Delta L = 1$ and a change in parity between the initial and final state. Since the He ground state is an S state with gerade parity the three body final state is ${}^1P^o$. Angular momentum is not a good quantum number for the individual electron, but the two electrons have to couple to angular momentum 1 with odd parity. This ${}^1P^o$ character of the 3-body final state shapes the momentum and angular distributions as will be discussed below in more detail.

The criterion for the validity of the dipole approximation is $k_\gamma r << 1$, where r is the typical size of the system (e.g. 1 a.u.). For single ionization there are detailed calculations including higher order contributions [1], confirming the validity of the dipole approximation at $E_\gamma < 1\,keV$. For double ionization no experimental evidence of any deviation from the dipole approximation have been found so far. Kornberg and Miraglia [2] performed the only theoretical study of double ionization beyond the dipole approximation. They find no deviation for the ratio of double to single ionization cross section R_γ and only small deviation in the angular distribution at 1 keV. The further discussion in this chapter will therefore be restricted to phenomena and arguments within the dipole approximation.

The three particles in the final state are determined by 9 momentum components. Due to momentum and energy conservation however only 5 of them are linearly independent. The double ionization process is therefore fully determined by a 5-fold differential cross section (FDCS). Sometime this is also called a triply differential cross section. In this notion the linearly independent polar (ϑ) and azimuthal (Φ) angle of the electrons are combined to a solid angle (Ω), the fully differential cross section is then noted as $d^3\sigma/dEd\Omega_1 d\Omega_2$. The dipole approximation results in a further symmetry axis in the final state (rotational symmetry around the polarization axis for linear light). This results in a further reduction to a only four-fold differential cross section. To measure such a cross section the experimentalist can freely choose which 5 out of the 9 momentum components to measure. Using dispersive [3–9], time-of-flight [10,11] electron spectrometers or advanced imaging techniques [12] several groups succeeded in detecting the momenta of both electrons without detection of the ion. Alternatively COLTRIMS has been used to measure the momentum vector of the ion in coincidence with one of the electrons [13–19].

Probability and Mechanisms of Double Ionization The absorption of a photon will lead in most cases to single ionization of the helium atom with the He^{1+} ion in the ground state. The two electron processes of ionization plus excitation and double ionization are in the order of a few % of the absorption cross section. They are solely a consequence of the electron-electron interaction. The absolute value of R_γ is settled today to an accuracy of a few % experimentally and theoretically. R_γ rises almost linearly from threshold,

reaches a maximum of 3.7 % at $E_\gamma = 200\,eV$ and slowly approaches the high energy asymptotic value of 1.67% (figure 14.1). Below 1 keV the precision experiments by Dörner et al. [20] and Samson et al. [21] are in good agreement with each other and supersede older experiments which where about 25% higher (see [20] for a comparison and discussion of these older experiments). In the high energy regime the pioneering work of Levin and coworkers reported an experimental value of $R_\gamma = 1.6 \pm 0.3\%$ at 2.8 keV of [22]. A measurement by Spielberger and coworkers [23] at 7 keV found R=1.72 ± 0.12% and thus confirmed that the high energy limit has been reached. A collection of the data and some of the theoretical results are shown in figure 14.1.

What are the "mechanisms" leading to the ejection of both electrons? This seemingly clear-cut question does not necessarily have a quantum mechanical answer. The word "mechanism" mostly refers to an intuitive mechanistical picture. It is not always clear how this intuition can be translated into theory and even if one finds such a translation the contributions from different mechanisms have to be added coherently to obtain the measurable final state of the reaction [24–26]. With these words of caution in mind, we list the most discussed mechanisms leading to double ionization:

1. **Shake-Off:** If one electron is removed rapidly (sudden approximation, nonadiabatic) from an atom or a molecule, the wave function of the remaining electron has to relax to the new eigenstates of the altered potential. Some of these states are in the continuum, so that a second electron can be "shaken-off" in this relaxation process. The overlap of the initial state $\Psi(k_1, k_2)$ with the continuum depends on the momentum k_1 of the primary electron [27]. I.e. the shake-off probability for electron 2 is a function of k_1. Photo-absorption in the dipole approximation selects the fraction of the initial state wave function where the initial bound momentum is equal to the continuum momentum $k_1 = \sqrt{2E_{\mathrm{exc}}}$. In the limit $k_1 \to \infty$ one obtains a shake-off ratio of $R_\gamma = 1.67\%$ for the best correlated initial state wave function [28,29], in perfect agreement with experiment (see figure 14.1). In coordinate space this limit corresponds to picking electron 1 at the nucleus. Due to this dependence of the shake-off probability on k_1, Compton scattering leads to a much smaller ratio R (see discussion in section14.1.3).
2. **Two-Step-One (TS1):** A simplified picture of TS1 is that one electron absorbs the photon and knocks out the second one via an electron-electron collision on its way through the atom [30]. A close connection between the electron impact ionization cross section and R_γ as function of the excess energy is seen experimentally [30] and theoretically [26], supporting this simple picture.

Thus the high energy value of R_γ is given by the shake-off process, the shape of the curve from threshold to a few hundred eV can be understood in analogy to electron impact. The rise at threshold like E_{exc}^{α} with the Wannier coefficient $\alpha = 1.056$ is identical for double photoionization [36] and electron

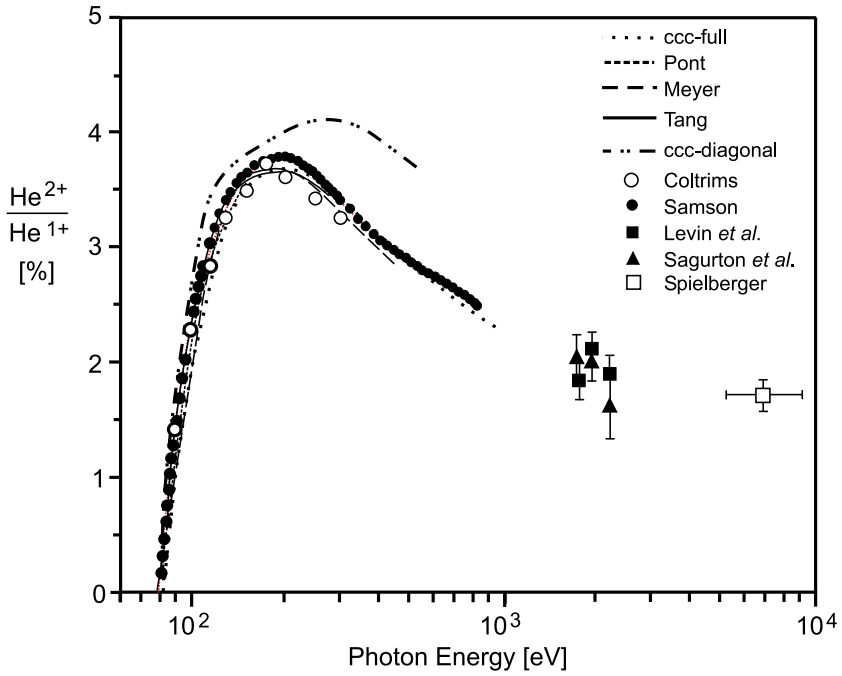

Fig. 14.1. Ratio of the total double to total single ionization cross section of Helium by photo-absorption. Open circles: COLTRIMS data [20], open square: COLTRIMS data for Photoionization only [23], full dots Samson et al. [21], full triangles [31], full square [32], dotted and dash dotted line [26], short dashed line [33], long dashed line [34], full line [35].

impact ionization [30]. It is a consequence of final state phase space density and is described by the Wannier threshold law [37]. If one fragments a system of charged particles with very little excess energy, the evolution of the many body-continuum wave function is governed by the saddle region of the potential energy surface in the continuum. The system does not carry any memory of the ionization process nor of the initial state it emerged from. The final state is however constraint by energy, parity and angular momentum conservation laws. For two electrons and one positive particle the Wannier configuration is simply given by the nucleus in the center between the two electrons, screening their repulsion. This configuration is however prohibited by the odd parity of the final state. Extending the description of the saddle region to fourth order allows a reasonable description of even the fully differential cross section up to about 20 eV [38,39,13,14].

Electron and Ion Momentum Distributions For single ionization the ion and electron momentum distributions are identically, since momentum

conservation requires back-to-back emission. An example for 80 eV linear polarized photons is shown in figure 14.7. The outer ring shows ions in the ground state, which exhibit a $\cos^2(\vartheta)$ dipolar distribution. The inner rings are excited ions, corresponding to the satellite lines in the electron energy spectrum. Figure 14.2 compares this to the momentum distributions of the He^{2+} ion and one of the electrons from double ionization. The nucleus clearly shows a dipolar emission pattern as a result of the absorption of the photon. This characteristics of the primary absorption process is completely washed out in the electronic momentum distribution. This highlights the fact, that the nucleus as the center of positive charge in the system always participates in the absorption of the photon. It is the electron-electron interaction which always is required for double ionization which smears out this reminiscent of the photons angular momentum in the momentum distribution of one single electron. A more detailed discussion of this problem can be found in [13,40,39,15].

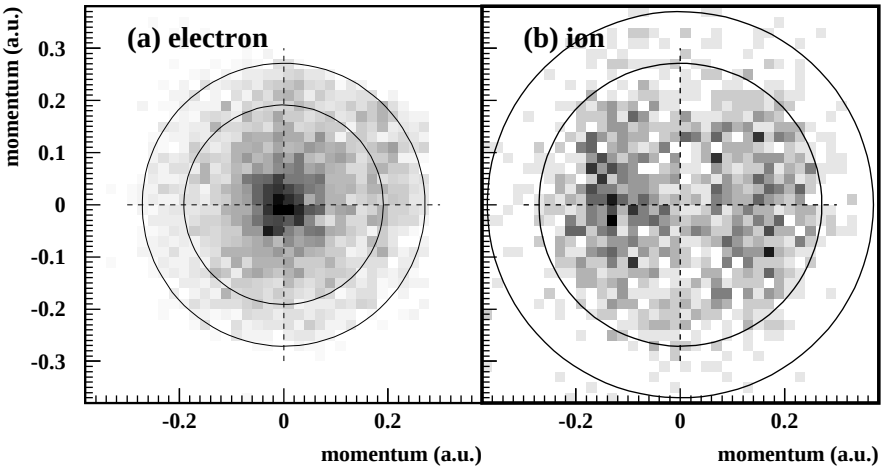

Fig. 14.2. Density plots of projections of the momentum distribution from double ionization of He by 80.1 eV linear polarized photons. Compare to figure 14.7 for the corresponding presentation for single ionization. The polarization vector of the photon is in the horizontal direction and the photon propagates in the vertical direction. a) The distribution of single electron momenta ($\mathbf{k_1}$ or $\mathbf{k_2}$). Only events with momentum components out of the plane of $-0.1 < k_{He2+} < 0.1$ are projected onto the plane. The outer circle locates the momentum of an electron which carries the full excess energy. (b) The recoil momentum distribution. The outer circle indicates the maximum calculated recoil momentum (from [13]).

The energy distribution of the electrons is almost flat up to a photon energy of about 100 eV, i.e. all energy sharings are about equally likely [41–

44]. Far from threshold, however, the electron energy distribution is extremely u-shaped. The fast electron in this case has a β parameter of almost 2 [1]. This indicates that at high photon energies the photon energy and angular momentum is absorbed predominantly by one electron, which in addition can be experimentally distinguished.

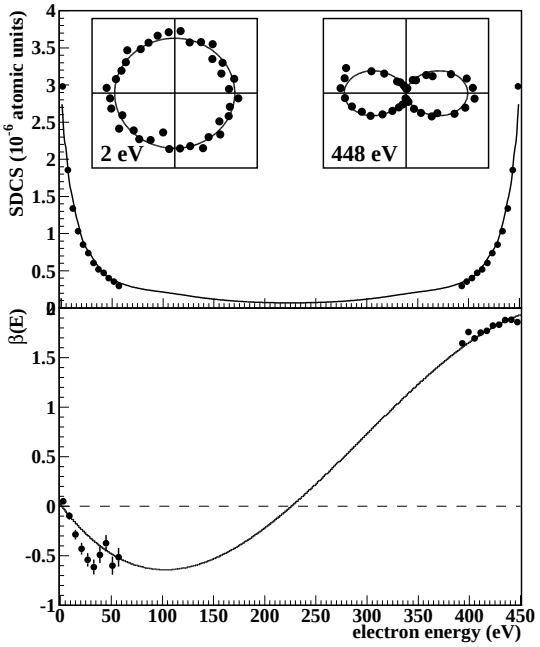

Fig. 14.3. Photo double ionization of He at $\hbar\omega = 529$ eV. a) SDCS $d\sigma/dE$. The line is the CCC calculation. The insets show the electron angular distribution $d\sigma^2/(d\Omega dE)$ at electron energies of $E = 2$ eV and 448 eV (the vertical axis is the light propagation), the line is obtained using equation 14.2. The experimental data are normalized to the CCC calculation. b) The asymmetry parameter β versus the electron energy. The full lines is a polynomial fit through points calculated in CCC theory.

Fully Differential Cross Sections The internal structure of the square of the correlated two electron continuum wave function is shown in figure

[1] The angular distribution of electrons and ions is given by

$$\frac{d^2\sigma(\vartheta,\phi)}{d\Omega} = \frac{\sigma}{4\pi}(1+\beta(\frac{3}{2}\cos\vartheta^2 - \frac{1}{2})). \tag{14.2}$$

$\beta = 2$ corresponds to a pure dipole distribution.

14.4. Neglecting the (small) photon momentum the vector momenta of ion and both electrons have to be in one plane. Figure 14.4(a) shows the electron momentum distribution in this plane for linear polarized light. The data are integrated over all orientations of the polarization axis with respect to this plane, the x-axis is chosen to be the direction of one electron. The structure of the observed momentum distribution is dominated by two physical effects. First the electron-electron repulsion leads to almost no intensity for both electron in the same half plane. Second, the $^1P^o$ symmetry leads to a node in the square of the wave function at the point $\mathbf{k_1} = -\mathbf{k_2}$ [45,3,46,47]. The corresponding data for left and right circular polarized light are shown in figure 14.4(b,c). They show a strong circular dichroism, i.e. a dependence on the chirality of the light. This might be surprising since the helium atom is perfectly spherical symmetric. Berakdar and Klar [48] first pointed out that for circular dichroism to occur it is sufficient that the direction of light propagation and the momentum vectors of the electrons span a tripod of defined handedness. This is the case if the two electrons and the light direction are non coplanar and the two electrons have unequal energy (see [49–51] for a detailed discussion and experimental results [10,17,9,52,53]).

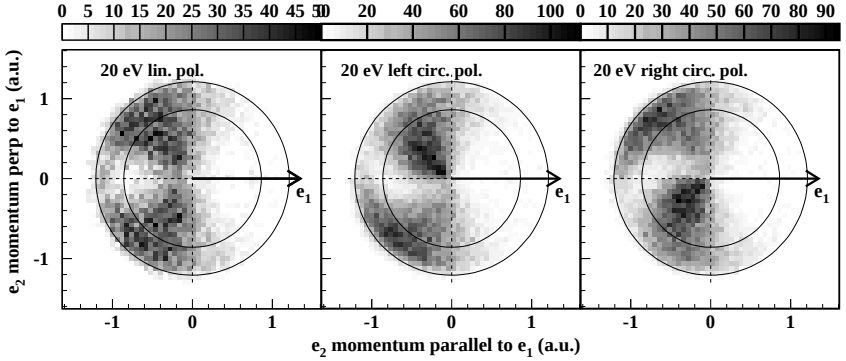

Fig. 14.4. Photo double ionization of He at 20 eV above threshold by linear (a) polarized light, left (b) and right (c) circular polarized light. Shown is the momentum distribution of electron 2 for fixed direction of electron 1 as indicated by the arrow. The plane of the figure is the momentum plane of the three particles. The data of (a) are integrated over all orientations of the polarization axis with respect to this plane. The figure samples the full cross sections, for all angular and energy distributions of the fragments. The outer circle corresponds to the maximum possible electron momentum, the inner one to the case of equal energy sharing. In (b) and (c) the light propagates into the plane of the figure, the electrons are confined to the plane perpendicular to the light propagation (from [54] and [18]).

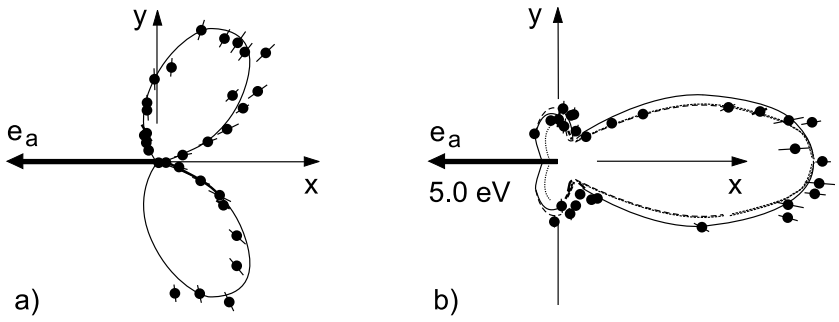

Fig. 14.5. FDCS of the He photo double ionization at (a) 20 eV and (b)52.9 eV excess energy. Electron a is indicated by the arrow, polarization horizontal. (a) $E_a = E_b = 10\,eV$, (b) $E_a = 5\,eV, E_b = 47,9\,eV$. Full line (a) fit with Gaussian correlation function (see text), (b) full line 3C from Maulbetsch and Briggs [55], dotted Pont and Shakeshaft [56], chain CCC [57](adapted from [3,4,58]).

The fully differential cross section for linear polarized light is obtained from figure 14.4(a) by fixing also the direction of polarization and then plotting the countrate along a circle. Data from the pioneering work of Schwarzkopf et al. [3] for equal energy sharing (corresponding to the inner circle in figure 14.4(a)) are shown in figure 14.5(a). Again the electron repulsion and the node for back-to-back emission is visible. The full curve shows a fit using a parametrization suggested by Huetz and others [45,47]. They have shown that within the dipole approximation the FDCS can be written as:

$$\frac{d^4\sigma}{dE_1 d\cos\vartheta_1 d\cos\vartheta_2 d\phi} \sim |(\cos\vartheta_1 + \cos\vartheta_2)a_g(E_1,\vartheta_{12}) + (\cos\vartheta_1 - \cos\vartheta_2)a_u(E_1,\vartheta_{12})|^2 \tag{14.3}$$

with two arbitrary complex functions functions a_u and a_g of the angle between the two electrons ϑ_{12} and the energy sharing. The amplitude a_u is antisymmetric under exchange of the electrons so that $a_u = 0$ for $E_1 = E_2$. The advantage of this approach is that it splits the cross section into a trivial part which describes the symmetry of the ${}^1P^o$ state and two functions of lower dimension which describe the three-body dynamics. For a_g a Gaussian with FWHM of 91 deg has been used in figure 14.5(a). For very unequal energy sharing a_u and a_g contribute and the selection rules allow for much richer pattern (figure 14.5(b) shows an example).

From equation 14.3 one can also read the 3 main selection rules [46] which impose restriction on the cross section:

1. For equal energy sharing back-to-back emission is forbidden (see node in figure 14.4). This holds for linear and circular polarization.
2. For equal energy sharing and linear polarized light $\vartheta_1 \neq 180 - \vartheta_2$ where ϑ denotes the polar angle of the electron to the polarization. This node

is a cone around the polarization axis and the back-to-back emission is part of this cone.
3. For all energy sharings not both electron can emerge perpendicular to the polarization ($\vartheta_1 = \vartheta_2 = 90^o$ is forbidden).

While at low energies the long range final state interaction shapes the FDCS, at very high energies one electron leaves fast (see figure 14.3) and clear traces of the shake-off and TS1 mechanism can be found in the angular distribution of the slow electron (see also [44,25]). The shake-off electron is expected to be isotropic or slightly backward directed with respect to the primary electron, while TS1 will yield 90^o between the two electrons. At 529 eV photon energy the electron angular distributions show a dominance of the shake-off mechanism for secondary electrons which have very low energy (2 eV) and display clear evidence that an inelastic electron-electron scattering is necessary to produce secondary electrons of 30 eV [19] (see figure 14.6).

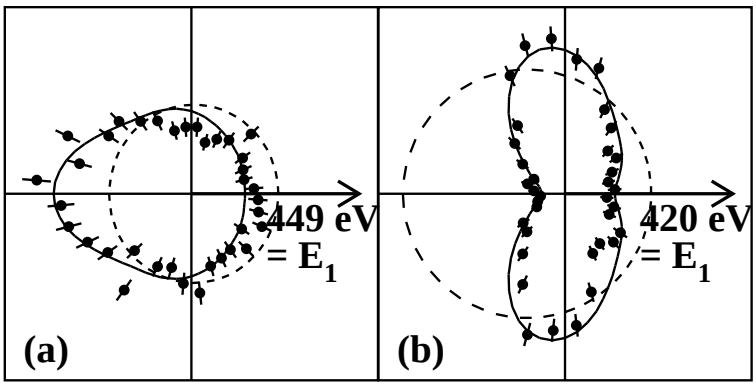

Fig. 14.6. FDCS of the He PDI at 529 eV photon energy. The primary photo electron 1 indicated by the arrow, the polarization is horizontal, the angular distribution of the complementary electron 2 with energy E_2 given by the symbols. a) $447 < E_1 < 450$ eV, $0 < E_2 < 3$ eV, b) $410 < E_1 < 430$ eV, $20 < E_2 < 40$ eV. a) shows the dominance of shake-off, the 90^o emission in b) indicates the importance of TS1 at this energy. The solid line shows the full CCC calculation, the dashed line is the shake-off only part of the CCC calculation (from [19]).

14.1.3 Double Ionization of Helium by Compton Scattering

At photon energies above 6 keV, the ionization cross section of helium by Compton scattering exceeds the photo-absorption cross section [59,60]. To experimentally determine the ratio of the total double to total single ionization cross section it is therefore necessary to detect not only the charge

state of the ions, but also determine wether they are created by absorption or Compton scattering. This can be done most easily by measuring the ion momentum. Ions from photo-absorption compensate the electron momenta and hence have comparably high momenta (section 14.1.2). In a Compton scattering event however the electron momentum is provided by the scattered photon while the ion core is only a spectator. As a consequence cold ions are produced (see section **??**). This has been used by Samson and coworkers to measure the single ionization Compton scattering cross section [61]. Spielberger and coworkers pioneered COLTRIMS to measure R for photo-absorption (R_γ) and Compton scattering (R_C) [23] separately (see also [62–64]). Figure 14.7 shows the measured He^{1+} momentum distribution created by about 9 keV photon impact. The circular rim results from high energetic ions from photo-absorption while the narrow peak at the origin are ions from Compton scattering. Since Compton scattering produces a continuum of electron energies, very high photon energies are necessary to approach the asymptotic shake-off limit [63]. The shake-off probability for Compton scattering is predicted to be 0.86% [63] and is not fully reached at 100 keV photon energy. R_C^∞=0.86% differs significantly from R_γ^∞=1.67% because high energy photo-absorption removes electrons with a high momentum component in the initial state, while Compton scattering samples the full initial momentum space. Up to today there are no differential experimental data on double ionization by Compton scattering available. In principle 8 degrees of freedom would have to be determined for a fully differential cross section. Such data are very desirable for the future since they complement (e,3e) and ion impact double ionization studies but avoid some of the problems since there are only 3 charged particles in the final state.

14.1.4 Double Ionization of H_2

Double ionization of H_2 is from the experimental as well as from the theoretical side much more challenging than atomic double ionization, since it is a 4-body problem. In most cases, however the electronic and nuclear motion can be decoupled (Born-Oppenheimer approximation) (see [65,66] for a theoretical discussion and [67] for the relationship of ion and electron energies). Within this approximation the four-body problem is reduced to the problem of two electrons moving and scattering in a two-center potential. Long after the two electron have left the molecule, the two protons will Coulomb explode. Since the molecular rotation is slow compared to the fragmentation one obtains the alignment of the internuclear axis at the instant of photo-absorption from the measured direction of the protons (axial recoil approximation) and the internuclear distance can be inferred from the proton energy (reflection approximation). This technique for measuring electron angular distribution with respect to the molecular axis for one electron is discussed in all detail in two other chapters of this book (see e.g. [68–74]).

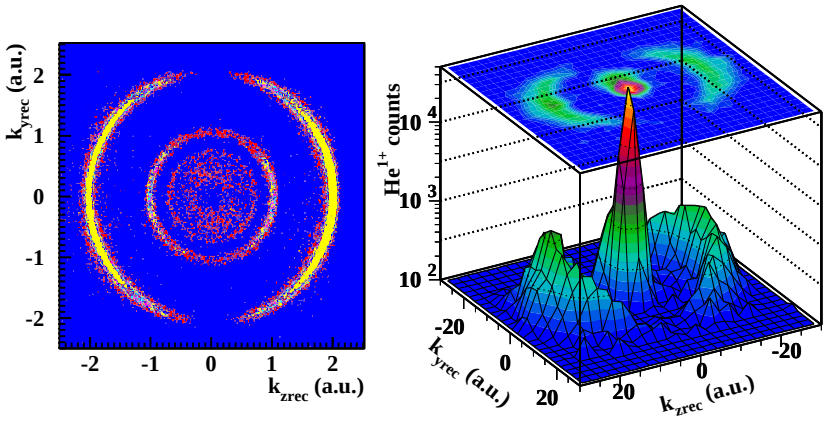

Fig. 14.7. Momentum distributions of singly charged ions created by 80 eV photons (photo-absorption only)(a) and 7 keV photons (outer rim: absorption, narrow peak: Compton scattering). The polarization is horizontal. See text.

The main difference between atomic and molecular photoionization is that in the atomic case the angular momentum is a good quantum number of the continuum electron wave function and within the dipole approximation only transition with $\Delta L = 1$ and a change in parity are allowed. For linear molecules angular momentum conservation also requires $\Delta L = 1$, but this is the angular momentum of the total wave function, including the nuclei. Total angular momentum is no longer a good quantum number of the electronic part of the wave function alone. Angular momentum can be exchanged between the electronic and nuclear wave function. The electron(s) escaping from the molecule can leave a rotating molecule behind (this rotation can be seen experimentally [75]). Hence for a linear molecule only the projection of the electronic angular momentum onto the molecular axis is a good quantum number of the electronic wave function. One may think of the angular momentum transfer between electron and nuclei as a scattering of the electron wave at the nuclei. At an electron energy of 1 a.u. and a typical distance of 0.7 a.u. between the molecule center of mass and the nucleus one can expect angular momentum exchange of up to a few a.u.. These higher angular momentum components in the electronic wave function allow for a rich structure already in the angular distribution of one electron in the molecule fixed frame [76–78]. For double ionization such higher momentum components are also predicted [79]

For H_2 double ionization in pioneering experiments Kossmann and Schmidt [80] measured the angular distribution of the protons, without detecting the electrons. They found a strong dependence of the double ionization cross section on the molecular orientation, i.e. a strong anisotropy of the heavy

fragments. No physical explanation for this observation has been reported so far. Reddish and coworkers studied the angular correlation between the two electrons without detection of the protons. They found a surprising similarity between He and H_2 (see figure 14.8 and references [81–83]). From these experiments it seems that the molecular effects one the two electron wave function are small at least for equal energy sharing. One reason for this similarity between He and H_2 is, that back-to-back emission of equal energy electrons is forbidden also for H_2 (see [84,79,85]). This is because in this case the sum momentum of the two electrons vanishes. There is no momentum coupling between electronic and nuclear wave function, the nuclei must have opposite and equal momenta and hence defined gerade parity. The additional selection rule prohibiting $\vartheta_1 = 180 - \vartheta_2$ which is valid for He does not hold for D_2 [84,85]. Due to a limited experimental angular resolution of the data in figure 14.8, this gives rise to an apparent filling of the node [83,85].

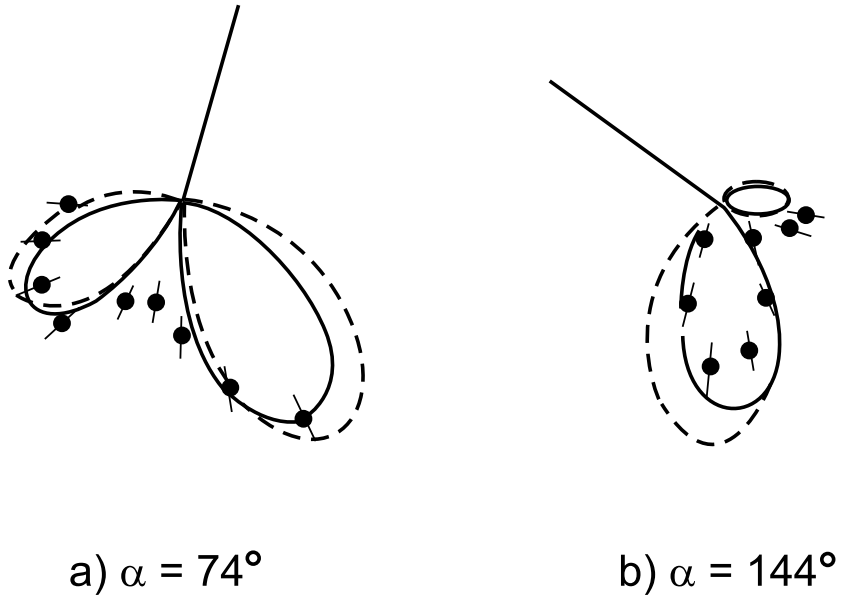

Fig. 14.8. FDCS for double ionization of D_2. Both electrons have 10 eV, the direction of the first electron is indicated by the arrow, both electrons are coplanar. The dashed line is a fit to the equivalent data for He with a gaussian correlation function of FWHM 91^o, the full line is FWHM=78^o. From [81]).

First kinematically complete experiment in which both electrons and both proton are detected in coincidence have been performed only very recently by Weber and coworkers [86,87]. Some of the physical effects which have been predicted by theory to become visible in such experiments are:

1. Contributions from higher angular momentum components to the two electron wave function [84,79] as discussed above.
2. Interference from the two centers in the H_2 molecule [88,79].
3. Different electron emission pattern for parallel and perpendicular orientation of the molecule to the polarization [79].
4. Dependence of the electron emission pattern on the internuclear distance, i.e. on the kinetic energy release [65,66]. This can be expected because the initial state electron wave function and in addition the scattering of the electron wave at the nuclei in the exit channel depend on the internuclear distance.

To explore this fascinating physics in the seemingly simple process of fragmentation of H_2 remains a major challenge to experiment and theory.

14.1.5 Conclusions and Open Questions

Decisive experimental and theoretical progress has been made concerning double ionization of Helium by photo-absorption. For ground state helium very good agreement between theory and experiment has been reached for experiment from $E_{\mathrm{exc}} = 100\,\mathrm{meV}$ to E_{exc}=450 eV. It is however unclear at which energies the dipole approximation will break down and which new features in the differential cross section can be expected beyond. Also the promise that photo double ionization can be used as a tool for correlation spectroscopy of the ground state [89,90] has not been kept. For further work in this direction comparison of ground state double ionization to double ionization from metastable excited states of helium or even spin polarized triplet state seems promising. Also the relation of double ionization by photons and charged particle impact (double ionization and transfer ionization) is still presently heavily discussed (see e.g. contribution by H. Schmidt-Böcking in this issue).

For double ionization by Compton scattering only total cross sections are available. Much work is required here on the experimental as well as on the theoretical side. Experiments are particulary hard since the cross section is only $10^{-26} cm^2$ and due to the photon in the final state there are 3 more degrees of freedom compared to photo-absorption. Again the close relationship between Compton scattering and ionization by a binary charged particle collision further fuel the interest in this subject.

Due to the rapid progress in multi particle imaging techniques the step from kinematically complete double ionization experiment in atoms to molecules is feasible experimentally. First theoretical results in this field are available already. The exciting prospects include the search for a breakdown of the Born-Oppenheimer approximation, for a coupling between electronic and nuclear wave function and for a dependence of the double ionization process on the internuclear distance.

References

1. J.W. Compton. *Phys. Rev.*, A47:1841, 1993.
2. M.A. Kornberg and J.E. Miraglia. *Phys. Rev.*, A52:2915, 1995.
3. O. Schwarzkopf, B. Krässig, J. Elmiger, and V. Schmidt. *Phys. Rev. Lett.*, 70:3008, 1993.
4. O. Schwarzkopf, B. Krässig, V. Schmidt, F. Maulbetsch, and J. Briggs. *J. Phys.*, B27:L347–50, 1994.
5. O. Schwarzkopf and V. Schmidt. *J. Phys.*, B28:2847, 1995.
6. P. Lablanquie, J. Mazeau, L. Andric, P. Selles, and A. Huetz. *Phys. Rev. Lett.*, 74:2192, 1995.
7. C. Dawson, S. Cvejanovic, D. P. Seccombe, T. J. Reddish, F. Maulbetsch, A. Huetz, J. Mazeau, and A. S. Kheifets. *J. Phys.*, B34:L525, 2001.
8. S Cvejanovic, J P Wightman, T J Reddish, F Maulbetsch, M A MacDonald, A S Kheifets, and I Bray. *J. Phys.*, B33:265, 2000.
9. K. Soejima, A. Danjo, K. Okuno, and A. Yagishita. *Phys. Rev. Lett.*, 83:1546, 1999.
10. J. Viefhaus, L. Avaldi, G. Snell, M. Wiedenhöft, R. Hentges, A. Rüdel, F. Schäfer, D. Menke, U. Heinzmann, A. Engelns, J. Berakdar, H. Klar, and U. Becker. *Phys. Rev. Lett.*, 77:3975, 1996.
11. J. Viefhaus, L. Avaldi, F. Heiser, R. Hentges, O. Gessner, A. Rüdel, M. Wiedenhöft, K. Wielczek, and U. Becker. *J. Phys.*, B29:L729, 1996.
12. A. Huetz and J. Mazeau. *Phys. Rev. Lett.*, 85:530, 2000.
13. R. Dörner, J. Feagin, C.L. Cocke, H. Bräuning, O. Jagutzki, M. Jung, E.P. Kanter, H. Khemliche, S. Kravis, V. Mergel, M.H. Prior, H. Schmidt-Böcking, L. Spielberger, J. Ullrich, M. Unverzagt, and T. Vogt. *Phys. Rev. Lett.*, 77:1024, 1996. see also erratum in Phys. Rev. Lett. 78. 2031 (1997).
14. R. Dörner, H. Bräuning, J.M. Feagin, V. Mergel, O. Jagutzki, L. Spielberger, T. Vogt, H. Khemliche, M.H. Prior, J. Ullrich, C.L. Cocke, and H. Schmidt-Böcking. *Phys. Rev.*, A57:1074, 1998.
15. H.P Bräuning, R. Dörner, C.L. Cocke, M.H. Prior, B. Krässig, A. Bräuning-Demian, K. Carnes, S. Dreuil, V. Mergel, P. Richard, J. Ullrich, and H. Schmidt-Böcking. *J. Phys.*, B30:L649, 1997.
16. H.P Bräuning, R. Dörner, C.L. Cocke, M.H. Prior, B. Krässig, A. Kheifets, I. Bray, A. Bräuning-Demian, K. Carnes, S. Dreuil, V. Mergel, P. Richard, J. Ullrich, and H. Schmidt-Böcking. *J. Phys.*, B31:5149, 1998.
17. V.Mergel, M. Achler, R. Dörner, Kh. Khayyat, T. Kambara, Y. Awaya, V. Zoran, B. Nyström, L.Spielberger, J.H. McGuire, J. Feagin, J. Berakdar, Y. Azuma, , and H. Schmidt-Böcking. *Phys. Rev. Lett.*, 80:5301, 1998.
18. M. Achler, V. Mergel, L. Spielberger, Y Azuma R. Dörner, and H. Schmidt-Böcking. *J. Phys.*, B34:L965, 2001.
19. A. Knapp, A. Kheifets, I. Bray, Th. Weber, A. L. Landers, S. Schössler, T. Jahnke, J. Nickles, S. Kammer, O. Jagutzki, L. Ph. Schmidt, T. Osipov, J. Rösch, M. H. Prior, H. Schmidt-Böcking, C. L. Cocke, and R. Dörner. *Phys. Rev. Lett.*, :submitted for publication, 2002.
20. R. Dörner, T. Vogt, V. Mergel, H. Khemliche, S. Kravis, C.L. Cocke, J. Ullrich, M. Unverzagt, L. Spielberger, M. Damrau, O. Jagutzki, I. Ali, B. Weaver, K. Ullmann, C.C. Hsu, M. Jung, E.P. Kanter, B. Sonntag, M.H. Prior, E. Rotenberg, J. Denlinger, T. Warwick, S.T. Manson, and H. Schmidt-Böcking. *Phys. Rev. Lett.*, 76:2654, 1996.

21. J.A.R. Samson, W.C. Stolte, Z.X. He, J.N. Cutler, Y. Lu, and R.J. Bartlett. *Phys. Rev.*, A57:1906, 1998.
22. J.C. Levin, D.W. Lindle, N. Keller, R.D. Miller, Y. Azuma, N.Berrah Mansour, H.G. Berry, and I.A. Sellin. *Phys. Rev. Lett.*, 67:968, 1991.
23. L. Spielberger, O. Jagutzki, R. Dörner, J. Ullrich, U. Meyer, V. Mergel, M. Unverzagt, M. Damrau, T. Vogt, I. Ali, Kh. Khayyat, D. Bahr, H.G. Schmidt, R. Frahm, and H. Schmidt-Böcking. *Phys. Rev. Lett.*, 74:4615, 1995.
24. Ken-ichi Hino, T. Ishihara, F. Shimizu, N. Toshima, and J.H. McGuire. *Phys. Rev.*, A48:1271, 1993.
25. S. Keller. *J. Phys.*, B33:L513, 2000.
26. A. Kheifets. *J. Phys.*, B34:L247, 2001.
27. T. Y.Shi and C. D. Lin. *Phys. Rev. Lett.*, , submitted for publication.
28. F.W. Byron and C.J. Joachain. *Phys. Rev.*, 164:1, 1967.
29. L.R. Andersson and J. Burgdörfer. *Phys. Rev. Lett.*, 71:50, 1993.
30. J.A.R. Samson. *Phys. Rev. Lett.*, 65:2861, 1990.
31. M. Sagurton, R.J. Bartlett, J.A.R. Samson, Z.X. He, and D. Morgan. *Phys. Rev.*, A52:2829, 1995.
32. J. C. Levin, G. B. Armen, and I. A. Sellin. *Phys. Rev. Lett.*, 76:1220, 1996.
33. M. Pont and R. Shakeshaft. *Phys. Rev.*, A51:494, 1995.
34. K.W. Meyer, J.L. Bohn, C.H. Green, and B.D. Esry. *J. Phys.*, B30:L641, 1997.
35. J.Z. Tang and I. Shimamura. *Phys. Rev.*, A52:1, 1995.
36. H. Kossmann, V. Schmidt, and T. Andersen. *Phys. Rev. Lett.*, A60:1266, 1988.
37. G.H. Wannier. *Phys. Rev.*, 90:817, 1953.
38. J.M. Feagin. *J. Phys.*, B28:1495, 1995.
39. J.M. Feagin. *J. Phys.*, B29:l551, 1996.
40. M. Pont and R. Shakeshaft. *Phys. Rev.*, A54:1448, 1996.
41. R. Wehlitz, F. Heiser, O. Hemmers, B. Langer, A. Menzel, and U. Becker. *Phys. Rev. Lett.*, 67:3764, 1991.
42. D. Proulx and R. Shakeshaft. *Phys. Rev.*, A48:R875, 1993.
43. M.A. Kornberg and J.E. Miraglia. *Phys. Rev.*, A48:3714, 1993.
44. Z.J. Teng and R. Shakeshaft. *Phys. Rev.*, A49:3597, 1994.
45. A. Huetz, P. Selles, D. Waymel, and J. Mazeau. *J. Phys.*, B24:1917, 1991.
46. F. Maulbetsch and J.S. Briggs. *J. Phys.*, B28:551, 1995.
47. L. Malegat, P. Selles, and A. Huetz. *J. Phys.*, B30:251, 1997.
48. J. Berakdar and H. Klar. *Phys. Rev. Lett.*, 69:1175, 1992.
49. J. Berakdar, H. Klar, A. Huetz, and P. Selles. *J. Phys.*, B26:1463, 1993.
50. J. Berakdar. *J. Phys.*, B31:3167, 1998.
51. J. Berakdar. *J. Phys.*, B32:L25, 1999.
52. A. Kheifets, I. Bray, K. Soejima, A. Danjo, K. Okuno, and A. Yagishita. *J. Phys.*, B32:L501, 1999.
53. A. Kheifets and I. Bray. *Phys. Rev. Lett.*, 81:4588, 1998.
54. R. Dörner, V. Mergel, H. Bräuning, M. Achler, T. Weber, Kh. Khayyat, O. Jagutzki, L. Spielberger, J. Ullrich, R. Moshammer, Y. Azuma, M.H. Prior, C.L. cocke, and H. Schmidt-Böcking. *Atomic processes in Plasmas*, AIP conference proceedings 443 (1998), 1998. Ed.: E. Oks, M. Pindzola.
55. F. Maulbetsch and J.S. Briggs. *J. Phys.*, B26:L647, 1994.
56. M. Pont and R. Shakeshaft. *Phys. Rev.*, A51:R2676, 1995.
57. A. Kheifets and I. Bray. *J. Phys.*, B31:L447, 1998.
58. J. Briggs and V. Schmidt. *J. Phys.*, 33:R1, 2000.

59. P.M. Bergstrom, Jr., K. Hino, and J. Macek. *Phys. Rev.*, A51:3044, 1995.
60. J.A.R. Samson, C.H. Green, and R.J. Bartlett. *Phys. Rev. Lett.*, 71:201, 1993.
61. J.A.R. Samson, Z.X. He, R.J. Bartlett, and M. Sagurton. *Phys. Rev. Lett.*, 72:3329, 1994.
62. L. Spielberger, O. Jagutzki, B. Krässig, U. Meyer, Kh. Khayyat, V. Mergel, Th. Tschentscher, Th. Buslaps, H. Bräuning, R. Dörner, T. Vogt, M. Achler, J. Ullrich, D.S. Gemmel, and H. Schmidt-Böcking. *Phys. Rev. Lett.*, 76:4685, 1996.
63. L. Spielberger, H. Bräuning, A. Muthig, J.Z. Tang, J. Wang, Y. Qui, R. Dörner, O. Jagutzki, Th. Tschentscher, V. Honkimäki, V. Mergel, M. Achler, Th. Weber, Kh. Khayyat, J. Burgdörfer, J. McGuire, and H. Schmidt-Böcking. *Phys. Rev.*, 59:371, 1999.
64. B. Krässig, R. W. Dunford, D. S. Gemmell, S. Hasegawa, E. P. Kanter, H. Schmidt-Böcking, W. Schmitt, S. H. Southworth, Th. Weber, and L. Young. *Phys. Rev. Lett.*, 83:53, 1999.
65. H. LeRouzo. *J. Phys.*, B19:L677, 1986.
66. H. LeRouzo. *Phys. Rev.*, A37:1512, 1988.
67. R. Dörner, H. Bräuning, O. Jagutzki, V. Mergel, M. Achler, R. Moshammer, J. Feagin, A. Bräuning-Demian, L. Spielberger, J.H. McGuire, M.H. Prior, N. Berrah, J. Bozek, C.L. Cocke, and H. Schmidt-Böcking. *Phys. Rev. Lett.*, 81:5776, 1998.
68. E. Shigemasa, J. Adachi, M. Oura, and A. Yagishita. *Phys. Rev. Lett.*, 74:359, 1995.
69. E. Shigemasa, J. Adachi, , K. Soejima, N. Watanabe, A. Yagishita, and N.A. Cherepkov. *Phys. Rev. Lett.*, 80:1622, 1998.
70. F. Heiser, O. Geßner, J. Viefhaus, K. Wieliczec, R.Hentges, and U. Becker. *Phys. Rev. Lett.*, 79:2435, 1997.
71. S Motoki, J Adachi, Y Hikosaka, K Ito, M Sano, K Soejima, G Raseev A Yagishita, and N A Cherepkov. *J. Phys.*, B33:4193, 2000.
72. A. Landers, T.Weber, I. Ali, A. Cassimi, M. Hattass, O. Jagutzki, A. Nauert, T. Osipov, A. Staudte, M. H. Prior, H. Schmidt-Böcking, C. L. Cocke, and R. Dörner. *Phys. Rev. Lett.*, 87:013002, 2001.
73. T. Weber, O. Jagutzki, M. Hattass, A. Staudte, A. Nauert, L. Schmidt, M.H. Prior, A.L. Landers, A. Bräuning-Demian, H. Bräuning, C.L. Cocke, T. Osipov, I. Ali, R. Diez Muino, D. Rolles, F.J. Garcia de Abajo, C.S. Fadley, M.A. Van Hove, A. Cassimi, H. Schmidt-Böcking, and R. Dörner. *J. Phys.*, B34:3669, 2001.
74. T. Jahnke, Th. Weber, A. L. Landers, A. Knapp, S. Schössler, J. Nickles, S. Kammer, O. Jagutzki, L. Schmidt, A. Czasch, T. Osipov, E. Arenholz, A. T. Young, R. Diez Muino, D. Rolles, F. J. Garcia de Abajo, C. S. Fadley, M. A. Van Hove, S.K. Semenov, N.A. Cherepkov, J. Rösch, M. H. Prior, H. Schmidt-Böcking, C. L. Cocke, and R. Dörner. *Phys. Rev. Lett.*, 88:073002, 2002.
75. H. C. Choi, R. M. Rao, A. G. Mihill, S. Kakar, E. D. Poliakoff, K. Wang, and V. McKoy. *Phys. Rev. Lett.*, 72:44, 1994.
76. J.L. Dehmer and D. Dill. *Phys. Rev. Lett.*, 35:213, 1975.
77. J.L. Dehmer and D. Dill. *J. chem. phys.*, 65:5327, 1976.
78. J.L. Dehmer and D. Dill. *Phys. Rev.*, A18:164, 1978.
79. M. Walter and J.S. Briggs. *J. Phys.*, B32:2487, 1999.
80. H. Kossmann, O. Schwarzkopf, B. Kämmerling, and V. Schmidt. *Phys. Rev. Lett.*, 63:2040, 1989.

81. T.J. Reddish, J.P. Wightman, M.A. MacDonald, and S. Cvejanovic. *Phys. Rev. Lett.*, 79:2438, 1997.
82. J.P. Wightman, S. Cveejanovic, and T.J. Reddish. *J. Phys.*, B31:1753, 1998.
83. T.J. Reddish and J. Feagin. *J. Phys.*, B32:2473, 1998.
84. M. Walter and J.S. Briggs. *Phys. Rev. Lett.*, 85:1630, 2000.
85. J.M. Feagin. *J. Phys.*, B31:L729, 1998.
86. T. Weber et al. , to be published.
87. T. Weber. , Dissertation, Frankfurt 2002.
88. I.G. Kaplan and A.P. Markin. *Sov. Phys. Dokl.*, 14:36, 1969.
89. V.G. Levin, V.G. Neudatchin, A.V. Pavlitchankov, and Yu.F. Smirnov. *J. Phys.*, B17:1525, 1984.
90. Yu.F. Smirnov, A.V. Pavlitchenkov, V.G. Levin, and V.G. Neudatschin. *J. Phys.*, B11:3587, 1978.